Steps dominate gas evasion from a mountain headwater stream

Gianluca Botter (gianluca.botter@dicea.unipd.it)
University of Padua https://orcid.org/0000-0003-0576-8847
Anna Carozzani
University of Padua
Paolo Peruzzo
University of Padua https://orcid.org/0000-0002-6712-9197
Nicola Durighetto
University of Padua https://orcid.org/0000-0002-6081-1580

Article

Keywords:

Posted Date: May 3rd, 2022

DOI: https://doi.org/10.21203/rs.3.rs-1558447/v1

Steps dominate gas evasion from a mountain headwater stream

Gianluca Botter[1*], Anna Carozzani[1], Paolo Peruzzo[1] and Nicola Durighetto[1]

[1]Department of Civil, Environmental and Architectural Engineering, University of Padua, via Marzolo 9 -35131- Padua (PD) - Italy

[*]To whom correspondence should be addressed;

E-mail: gianluca.botter@dicea.unipd.it.

April 2022

Abstract

Step-and-pools are dominant morphologic traits of high-energy streams, where climatically- and biogeochemically-relevant gases are processed, transported to downstream ecosystems or released into the atmosphere. Yet, capturing the signature of the small-scale morphological complexity of channel forms on large-scale river outgassing represents a fundamental unresolved challenge. Here, we combine theoretical and experimental approaches to assess the contribution of localized steps to the gas evasion from river networks. The framework was applied to a representative, $1\,km$-long mountain reach in Italy, where carbon dioxide concentration drops across several steps and a reference segment without steps were measured under different hydrologic conditions. Our results indicate that local steps lead the reach-scale outgassing, especially for high and low discharges. These findings suggest that step-pools are key missing components of existing scaling laws used for the assessment of gas fluxes across water-air interfaces. Therefore, global evasion from rivers may differ substantially from previously reported estimates.

Introduction

River networks transport, process and release a multitude of chemical substances, which are relevant to the biogeochemical functioning of stream ecosystems and eventually affect the fragile interconnections of the land-water-climate nexus[1–4]. In particular, headwater streams are important greenhouse gas sources

to the atmosphere, owing to enhanced input of dissolved matter from the surrounding landscape and high exchange rates across water-air interfaces. Consequently, quantifying gas emissions from upland freshwater systems is regarded as an important scientific challenge with multi-faced implications for a broad range of disciplines including ecology, biology and climate sciences[5–8].

Riffles represent a distinctive trait of most rivers worldwide[9]. In high-gradient streams, where the granulometry is varied, riffles frequently give rise to sequences of step and pools in which local hydraulic discontinuities of the water flow are observed. Step-pool bedforms are thus widespread in different regions of the globe, including humid areas, desert ephemeral systems, semiarid environments and alpine settings[10,11]. The important role of steps in regulating fluvial sediment transport and channel morphology has been extensively studied[12–19], but systematic knowledge about their contribution to gas exchange between freshwater systems and the atmosphere remains elusive.

Several authors have argued that waterfalls, riffles, steps and cascades might promote gas exchange with the atmosphere, owing to the enhanced turbulence and air entrainment that are typically observed in correspondence of abrupt discontinuities of the flow field[7,20–28]. However, available empirical data about the outgassing produced by individual steps or cascades is relatively limited. Cirpka et al.[20] and Natchimuthu et al.[29] have used tracer injections to demonstrate that the presence of cascades and waterfalls significantly increases the reareation coefficient in a set of tens-of-meters long river reaches located in Switzerland and Sweden. More recently, Leibowitz et al.[30], Vautier et al.[31] and Schneider et al.[32] have shown that mass evasion within channel stretches that contain waterfalls is enhanced, causing a loss of carbon dioxide (CO_2) or injected tracers within relatively short distances in the range of 15% to 50% of the initial mass. However, spatial patterns of gas evasion were typically monitored at relatively coarse spatial resolutions (i.e. some tens of meters), and empirical observations at scales comparable to the step size are much rarer (see ref.[31]). High resolution data, instead, represent a powerful means to reduce the uncertainty in the characterization of small-scale patterns of stream outgassing, and enable more robust assessments of gas evasion produced by local hydro-morphologic heterogeneities of rivers[33].

Existing studies aimed at quantifying the relative contribution of cascades to the total stream outgassing typically rely on spatial patterns of gas concentration within river reaches that contain steps or waterfalls[30–32]. These patterns, however, inherently mirror the unique morphologic characteristics of the case studies selected for the analysis. Consequently, the existing estimates can not be easily upscaled or extrapolated to different contexts. In other instances, gas evasion produced by steps and cascades was investigated through the analysis of the underlying mass transfer rate, k[27,29,31,34]. Though, this metric can be strongly biased when the spatial resolution of the available data is insufficient[35]. In fact, the mean value of k in a given stream portion is not able to capture internal peaks of gas transfer that might be observed when the size of the fluid volume responsible for most of the evasion is smaller than the measurement resolution - as in the presence of a falling jet (P.P., N.D. and G.B., in prep.).

Owing to these theoretical and practical limitations - in spite of the growing awareness of the importance of local heterogeneity of the flow field in water-air gas exchange - the relative contribution of steps to the total outgassing in morphologically-complex reaches is not fully clear. This study aims at filling this gap by developing a theoretical and experimental framework for the study of gas emissions in heterogeneous streams. The approach was applied to a high-gradient channel in the Italian Alps where water CO_2 concentrations were measured across 19 natural and artificially-created steps, and along a reference turbulent segment without steps. The main innovation of the experimental setup is that we capitalize on direct CO_2 records gathered under different discharge conditions, without relying on Schmidt-number scaling, which is problematic in case of bubble-mediated transport of the type observed downstream of steps and cascades[25,34,36,37]. The major theoretical advance, instead, pertains the development of a modular and scalable metric for disentangling the contribution of turbulent segments and local steps to the total stream outgassing. The scalability of this metric was exploited to assess the role of local steps in the reach-scale outgassing, taking into account both the temporal variations of the discharge and the morphological characteristics of the river bed.

Concentration damping in streams

While we recognize that the morphological complexity of rivers might not fit perceptual models of the type proposed here, we conceptualize high-gradient stream networks as a heterogeneous sequence of two types of elements: steps and segments (Figure 1b). Local steps are point-wise hydraulic discontinuities of the flow, generated by a drop of the riverbed Δh higher than the typical flow depth ($\Delta h > 10\,cm$ in this case). In such circumstances, the presence of a falling jet promotes air entrainment, bubbles and foaming which enhance gas exchange with the atmosphere. Turbulent segments, instead, are continuous, relatively regular river stretches located in between pairs of steps, in which the flow is gradually varied. Therein, turbulence and gas-exchange are promoted by heterogeneities of the velocity field, which are in turn produced by e.g. hurdles, stones, bends and bed roughness.

A proper evaluation of the role of local steps in river gas evasion requires the definition of a metric capable of objectively determining the separate contribution to the outgassing of steps and turbulent segments. To this aim, we utilize the concept of concentration damping, which is a dimensionless, scalable measure of gas evasion applicable to individual steps, single segments or composite heterogeneous channels. Under steady state conditions, the $1D$ spatial pattern of the concentration C of a dissolved gas advected downstream (x direction) and evaded into the atmosphere is exponentially decreasing with a spatially-heterogeneous decay rate (Methods):

$$C(x) = C_a + (C_0 - C_a) \exp\left[-\int_0^x \frac{K(x')}{u(x')} dx'\right] = C_a + (C_0 - C_a]) \exp[-f(x)] \quad (1)$$

where $C(x)$ is the concentration in the position x along the streamline, C_0 the concentration in the upstream section ($x = 0$), $u(x)$ the water velocity, $K(x)$ the exchange rate (here defined as the gas transfer velocity k scaled to the water depth) and f is the exponential damping factor (hereafter damping factor). Starting from its definition as given in Equation (1), f can be expressed as the product between an effective exchange rate along the stretch $(0, x)$, $K_{eq}(x)$, and the corresponding water travel time $\tau(x)$, i.e. $f(x) = K_{eq}(x)\tau(x)$ (Methods). In particular, the damping factor of a continuous channel segment (say, c_i) of length ℓ_i can be written as:

$$f_{c_i}(\ell_i) = K_{c_i} \tau_{c_i} \,, \quad (2)$$

where $\tau_{c_i} = \int_0^{\ell_i} 1/u(x) dx$ is the travel time spent by water parcels in the segment (measurable via tracer experiments) and K_{c_i} the effective exchange rate therein.

Analogously, the damping factor of the step s_i, f_{s_i}, can be expressed as:

$$f_{s_i}(\Delta h_i) = K_{s_i} \, \tau_{s_i} \ , \quad (3)$$

where K_{s_i} is the effective exchange rate within the step i and τ_{s_i} the corresponding travel time. The notation emphasizes that f_{s_i} should depend on the step height Δh_i, which drives the amount of energy dissipated by the water flow and the ensuing outgassing process. In the case of steps and cascades, it is practically unfeasible to separately measure τ_{s_i} and K_{s_i}. Nevertheless, step exchange rates (K_{s_i}) are expected to be very high owing to the local increase of energy dissipation and the enhanced air entrainment in correspondence of the falling jet[20,38–40]. Consequently, f_{s_i} could be comparable to (or even larger than) f_{c_i} in many settings, in spite of the "local" nature of the outgassing process in correspondence of the steps (i.e., $\tau_{s_i} < \tau_{c_i}$).

The damping factor is additive and commutative (Methods), thereby implying that the value of f for a series of segments (steps) can be calculated as the sum of the damping factors associated to the individual segments (steps) involved, regardless of their specific order (SI). Consequently, we can evaluate the relative contribution to the total outgassing induced by all the steps embedded in a focus reach (or river network) using the dominance ratio r, which is defined as the ratio between the damping factor of the steps (f_s) and the damping factor of the segments (f_c) of that reach (see Figure 1b and SI):

$$r = \frac{\sum_i f_{s_i}}{\sum_i f_{c_i}} = \frac{f_s}{f_c}. \quad (4)$$

In Equation (4), f_c (f_s) is expressed as the sum of the damping factors of all the segments (steps) included in the reach (figure 1b and Methods). If the

dominance ratio is equal to unity, then the steps and the continuous segments of the focus reach provide an equal contribution to the total river outgassing (meaning that the gas concentration damping produced by a sequence of steps would be the same as the concentration damping produced by the turbulent continuous segments without the steps). Likewise, if $r > 1$ ($r < 1$) then the steps proved a larger (smaller) contribution to the outgassing as compared to the contribution generated by the continuous turbulent stretches. Crucially, r is not affected by the specific order according to which segments and steps are arranged, but only depends on key geometrical and hydraulic features of river networks (e.g. step height/spacing, segment slope).

Steps dominate reach-scale gas evasion

The empirical estimates of the damping factors of the steps and the reference segment belonging to the focus reach considered in this paper are summarized in Fig. 2. In the reference segment, the damping factor f_{c_r} ranged from 0.1 (corresponding to approximately 10% of excess mass removed) to 0.32 (25% of excess mass removed), depending on the underlying flowrate, Q. The non monotonous dependence of f_{c_r} on Q was explained by the interplay between two important drivers of gas transfer across water-air interfaces: i) the mean flow velocity, which is positively correlated with the outgassing velocity and is an increasing function of Q (Fig S4); and ii) the ratio between exchange area and water volume, which is proportional to the exchange rate but decreased with Q in the reference segment (Table S3). Consequently, f_{c_r} peaked for intermediate discharges.

The estimated values of the damping factor in the natural and artificially-generated steps (Methods and SI), instead, ranged from 0.03 to 0.27. In most cases f_{s_i} had the same order of magnitude of f_{c_r}, demonstrating that a local step may originate the same outgassing produced by turbulent river segments with a length of tens of meters. Interestingly, f_{s_i} showed an almost linear dependence on the step height. The increase of the damping factor with the step height was explained by the fact that the turbulent energy dissipated by the plunging jet - which drives the outgassing process - increases with Δh_i. However, the physical reasons underpinning the linear dependence of f_{s_i} on Δh_i are less trivial, and deserve more investigations. Instead, f_{s_i} was found to be statistically independent on the discharge Q (SI). This is because the rate of gas exchanged through the step is chiefly determined by the turbulent kinetic energy for unit weight of fluid dissipated by the cascade, which is well approximated by the potential energy loss across the drop (Δh_i) regardless of the underlying discharge conditions.

The natural steps, where CO_2 production was impeded by manually scouring and removing all the biofilm from the river bed and the downstream pool prior to each measurement, showed a behaviour which was essentially undistinguishable from that of the artificially created steps, suggesting that the procedure used for simulating the steps with pipe diversions didn't introduce significant biases

in our analysis. The dependence of f_{s_i} on the step height (Δh_i) in natural steps covered with the plastic film was in line with that observed for the other steps, while the underlying absolute values were slightly lower - likely because in this setting the falling jet adhered to the plastic film, thereby reducing the reaeration rate and the gas evasion in the covered steps.

The ratios between f_s and f_c in the three reference reaches analyzed in this study (the reaches A and B, and the virtual reach A^*, see Methods), were found to be in the range $[0.9 - 4.3]$, depending on the underlying discharge level and the specific reach analyzed. These values were calculated taking into account the number and heights of the steps within each reach, and using a linear empirical function to link f_{s_i} to Δh_i as suggested by our experimental data (dashed line in Figure 2a). Interestingly, most of the gas evasion induced by the steps was associated to the smallest drop heights. In fact, about 60 % of f_s was contributed by steps with heights smaller than $35\,cm$ (SI). Provided that f_s turned out to be independent on Q while f_c peaked for intermediate discharge levels, r had a non monotonic dependence on Q, with higher values observed for low and high streamflow conditions. Remarkably, in all the settings analyzed r was systematically larger than (or close to) unity, thereby indicating that the contribution to gas evasion provided by the steps in the Valfredda creek was remarkable, particularly during low-flow and high-flow conditions.

The temporal changes of the dominance ratio - as induced by the hydroclimatic fluctuations experienced by the focus reach from July 2021 to November 2021 - are shown in Fig. 3b and 3c. The temporal pattern of r was reconstructed from the underlying simulated discharge variations (Methods), using the empirical relationship between r and Q shown in Figure 3a. Our results clearly indicate that r remained consistently above unity during the whole monitoring season for the three reference river reaches analyzed. The highest values of r were observed during high flow conditions. The resulting average values of the dominance ratio during the whole monitoring period were equal to 2.4 (for the reach A), 2.5 (for the reach B) and 3.2 (for the reach A^*). We conclude that the outgassing from the study reach of the Valfredda was largely dominated by the local evasion induced by step and pools during the summer and early fall of 2021.

Implications for large-scale studies

On practical grounds, objectively decomposing morphologically-complex channels of the type investigated here into segments and steps may not be straightforward. Here, steps were identified in correspondence of sharp drops in the active river bed, with heights that exceed $10\,cm$. In our experimental set-up, drops of this type gave rise to aerated falling jets followed by bubbles and/or foaming in the downstream pool, thereby enhancing gas exchange with the atmosphere. In some cases, however, vertical drops could be very small and/or involve only a portion of the active riverbed, creating spatially heterogeneous hydrodynamic conditions which are quite difficult to describe. These hybrid elements were not

considered as actual steps in this paper - and their contribution to gas emissions was neglected accordingly. Furthermore, owing to spatial heterogeneity of key hydro-morphological characteristics such as slope, discharge and riverbed composition/roughness, the continuous emissions in all the segments belonging to the study reach might not be perfectly represented by the behaviour of the reference segment as postulated by the upscaling procedure proposed in this paper. Nevertheless, in spite of all these limitations and the inherent local nature of our study, we believe that the results shown here can be of general validity and properly describe the order of magnitude of the processes involved, as long as the morphology of the mapped steps is in line with previously published data gathered in different regions of the World[41–45]. Therefore, the important contribution of small-height steps to the total outgassing observed in the Valfredda is expected to emerge in many high-slope settings, where step and pool bedforms dominate the channel morphology.

Our study revealed that the footprint of gas emissions produced by local steps do not vanish at the reach scale, owing to the pronounced concentration damping in correspondence of each step and the high frequency of step-and-pools typical of steep mountain rivers. This key finding prescinds from the precise value taken by the dominance ratio, which might vary from site to site depending on local morphologic and hydraulic features (e.g. channel slope, substrate, step frequency). Besides, the weak dependence of r on the specific reach used for the upscaling suggests that the dominance ratio could be a relatively smooth function of space, as long as it integrates the effect of a sufficiently large number of steps. This feature makes this dimensionless metric suitable to be scaled across space or extrapolated along river networks, e.g. across different channels with similar morphologic characteristics.

The damping factors and the dominance ratio quantify the potential outgassing of different stream elements, whereas the actual value of evaded mass does depend on the spatial correlation between the sources of matter along the stream and the spatial patterns of evasion, here encapsulated by the damping factor[24]. Given the local nature of gas emissions from step and pools, cascades and waterfalls, these geomorphic elements could act as important emission hotspots, where the excess mass transported downstream by the flow is quickly released into the atmosphere (e.g. refs [22,26,30]). Therefore, there could be a significant amount of outgassed mass in correspondence of steps, which could be essentially undetectable because of the very short distances traveled from the input (or production) site to the evasion point.

Step-and-pools represent crucial morphologic components of high-energy streams, as they drive the transport of matter downstream, and regulate physical or chemical exchanges at the interface with the landscape and the atmosphere. Consequently, a proper characterization of the step frequency and geometry is an important prerequisite for a robust assessment of gas evasion from channel networks. We conclude that key geomorphological factors other than spatially-averaged characteristics of a reach (e.g. mean slope, mean velocity) should be properly incorporated in existing scaling laws currently in use for the prediction of global-scale gas evasion from freshwater systems[5,25,46–48]. In heterogeneous

high-energy streams, in fact, different stretches characterized by the same mean slope and velocity could lead to highly variable gas evasion rates depending on their internal configuration. For instance, the $13\,m$ reference segment considered in this study was able to evade - through a total elevation drop of $1.4\,m$ - approximately $8\,\%$ to $27\,\%$ of the available excess mass, depending on the underlying discharge rate. If the same mean slope and elevation drop were obtained by combining nearly horizontal segments with two steps (SI), the damping factor would be much higher (from $30\,\%$ to $250\,\%$ higher than that observed in the reference segment), with a percentage of excess mass evaded close to $35\,\%$. The example indicates that small-scale morphological traits of rivers, such as steps, riffles, cascades or waterfalls can significantly enhance gas exchange at the water-air interface and - therefore - need to be properly accounted for when observed patterns of gas evasion are extrapolated outside the specific context where these data were gathered[35]. Better characterizing the local morphological traits of streams that regulate the mass exchanged through water-air interfaces at regional or global scales could help us to constrain the budget of focal chemical species (e.g. carbon, oxygen, nitrogen) relevant to the water-land-climate system.

Methods

Damping factor

The equation governing the spatial patterns of gas concentration in a one-dimensional system with a curvilinear coordinate x aligned with the main flow direction, under the assumptions of stationarity (constant flow rate and time-invariant gas concentrations), no dispersion, no lateral input, absence of internal gas production reads:

$$u(x)\frac{dC(x)}{dx} + K(x)[C(x) - C_a] = 0\,, \tag{5}$$

where $u(x)$ is the local velocity in the streamline direction, C_a the atmospheric concentration, $C(x)$ the local water gas concentration, $K(x)$ the local, spatially variable exchange rate, which is equal to the mass transfer rate k scaled to the mean water depth. Crucially, the exchange coefficient K embeds the coupled effects of the mass transfer induced by the turbulence of the flow and that associated to gas transport mediated by bubbles and foams (if any, see ref[49]). The solution of Equation (5) is given by Equation (1) in the main text. Therein, the exponential damping factor can be expressed as:

$$f(x) = \int_0^x \frac{K(x')}{u(x')}dx' = \int_0^{\tau(x)} K(t')dt' = K_{eq}(x)\tau(x)\,, \tag{6}$$

where $K_{eq}(x)$ is a weighted spatial average of K in the stretch from 0 to x and $\tau(x) = \int_0^x 1/u(x)dx$ is the corresponding transit time - the time necessary to

travel from 0 to x (SI). Thanks to Equation (1), f_c - the damping factor of an ideal channel stretch of lenghth L composed by all the continuous segments of the focus reach - could be expressed as:

$$f_c = ln\left[\frac{C_0 - C_a}{C_L - C_a}\right], \tag{7}$$

where C_0 and C_L are the gas concentrations in the upstream ($x = 0$) and downstream ($x = L$) sections of the reach. Operationally, given the practical impossibility of measuring f_{c_i} within all the segments belonging to the focus reach, f_c was calculated based on the value of the damping factor of a representative segment (see below) with length ℓ_r, f_{c_r}. The latter was estimated from Equation (7) through direct gas concentration measurements as:

$$f_{c_r} = ln\left[\frac{C_0 - C_a}{C_{\ell_r} - C_a}\right], \tag{8}$$

where C_0 and C_{l_r} are the concentrations in the upstream and downstream sections of the reference segment. Then, f_c was calculated from f_{c_r} as:

$$f_c = f_{c_r}\frac{L}{\ell_r}, \tag{9}$$

exploiting the additivity of f_{c_i} across multiple segments and assuming that the exchange rate in the reference segment is equal to the average value of K across all the segments contained in the focus reach (SI).

Similarly, f_{s_i} was calculated from Equation (1) as:

$$f_{s_i} = ln\left[\frac{C_{u_i} - C_a}{C_{d_i} - C_a}\right], \tag{10}$$

where C_{u_i} and C_{d_i} represent the water gas concentration upstream and downstream of the step i. The damping factor of a sequence of N steps was then evaluated summing up the damping factors of all the individual steps f_{s_i} (i.e. $f_s = \sum_i f_{s_i}$, see SI), as in Equation (4) of the main text.

Study site and focus reach

The study site selected in this paper is a step-pool channel of the Rio Valfredda, a high-gradient headwater catchment of the Piave river basin, in the Italian Alps[35,50]. The climate of the site is typically alpine: precipitation is relatively high throughout the year (annual rainfall > 1400 mm), with significant snowfall during winter and melting in spring[51]. The selected reach is $1.36\,km$ long, and its elevation ranges from 1911 to 1720 m a.s.l., with a mean slope of 0.14 m/m (Fig. 1**a**). The reach was selected because of its accessibility and the significant CO_2 concentrations observed therein. The river bed is steeper in the upstream part, where it flows southwards. Then, the reach runs south-east across some pastures and a mixed larch-spur forest. The reach is fed at its source by a

groundwater spring. The discharge weakly increases downstream, owing to the interplay between the losing bed and the hillslope lateral input. The stream bed is silty and dominated by boulders, cobbles and wooden logs of different size that originated several steps and pools. About $300\,m$ upstream of its confluence with the Valfredda, the channel was almost inaccessible due to the presence of a landslide and several fallen trunks. Therefore, the analysis was concentrated in the upper portion of the channel (reach A, with a total length $L_A = 1.06\,km$ (blue line in Fig. 1**a**)). To capture the footprint of the bed geomorphology on gas evasion, the reach A was decomposed into 270 segments and 271 steps (Fig. 1**b**). A representative segment with a slope (discharge) similar to the mean slope (mean discharge) of the continuous segments within the study reach was identified in the middle part of the reach (46°22'50"N, 11°49'39"E, see Fig. 1**a**). This representative segment has an average slope $i_{c,r}$ of 0.108 m/m and a length ℓ_r of $13\,m$ (inset of Fig. 1**a** and 1**c**).

Discharge measurements

We performed several volumetric measurements of the discharge rate, Q, at the two end points of the representative segment. This was done recording the filling time of a graduated tank in correspondence of the upstream and downstream section of the representative segment. We performed 10 measurements between July and October 2021, with observed discharge values between 0.2 and 3.2 l/s (see Table S1). Each measurement was the average among at least 5 different replicas performed in both the locations within one hour.

Travel time measurements and estimation of the relevant hydraulic properties

The water travel time along the representative segment, τ_{ℓ_r}, was measured through instantaneous injections of a diluted sodium chloride (NaCl) solution in the upstream cross section of the segment. The temporal variations of specific conductivity at the outlet of the segment were then measured using a multi-parameter sonde (YSI EXO2). The travel time was recorded both under natural conditions and after having covered the stream bed with the plastic film (Fig. S2 and S3). The longitudinal mean velocity, u, was estimated as the segment length, ℓ_r, divided by the observed travel time. The procedure allowed us to verify that the mean velocity along the reference segment was not significantly impacted by the presence of the plastic film. Moreover, after having covered the river bed with the plastic film, we also measured the mean width, W, and water depth, H of the flow. This was done by taking spatial averages of the local values observed in different cross sections along the segment. The obtained hydraulic geometry scaling relationships (Fig. S4) were found to be in line with the relationships proposed in the literature for mountain streams[8], thereby suggesting that the flow conditions in place during the CO_2 measurements were nearly-natural.

CO_2 concentration measurements

Paired upstream and downstream CO_2 concentration measurements were taken in the representative segment and in 19 steps (see SI), using a membrane-based NDIR sensor, the MiniCO$_2$™ designed by ProOceanus Systems Inc., Bridgewater, Canada. The instrument has a tubular shape, $370\,mm$ long and $53.4\,mm$ in diameter, and uses infrared detection to measure the partial pressure of dissolved CO_2. Once the internal gas is fully equilibrated with the surrounding water (typically 10-15 min after the deployment), NDIR measurement on the equilibrated internal gas is taken at a wavelength of $4.26\,\mu m$ close to the absorption band of CO_2 at a controlled optical cell temperature. The time of deployment in a given position ranged from 30 to 90 minutes. To eliminate the confounding effect of high-frequency fluctuations in the recorded CO_2 signal of the MiniCO$_2$™ sensor (see Figure 1c-1e for an example), at least 20 minutes of continuous measurements at steady-state were gathered, from which we estimated the probability density function of CO_2 concentrations and the related mean. Steady-state conditions were pre-identified based on the temporal patterns of the long-term average of the signal. The steady state mean was then taken as representative of the equilibrium carbon dioxide concentration in water (Fig. S8 and S9). Paired upstream-downstream concentrations were gathered within 120 mins from each other, so as to reduce as much as possible spurious effects induced by diel variations of water CO_2 concentration.

Estimating f_{s_i} AND f_{c_r}

In this study the damping factors were evaluated on a purely experimental basis. The damping factor of individual steps f_{s_i} was estimated from upstream/downstream CO_2 measurements via Equation (10), considering three different step types: i) 11 simulated steps, which were created forcing the water into pipes and then letting the water flow hit a covered portion of channel bed from a given height, so as to reproduce the behaviour of a falling jet of a natural drop with the desired Δh (Fig. 1**d** and S5); ii) 4 covered steps, obtained by folding natural steps with a thin plastic film, which was carefully shaped around the actual channel bed in the ramp, the step and the downstream pool (Fig. S6**e**); iii) 4 natural steps belonging to the focus reach (Fig. 1**e** and S6**f**), which were scoured to remove the existing biofilm prior to each measurement. These precautions allowed us to eliminate the effect of CO_2 production in all the analyzed steps, while assuring natural hydraulic conditions in all the measured steps. Further details on the experimental setup are available in SI.

As per the estimate of the damping factor in the reach segments, owing to the practical impossibility to quantify the outgassing within all the segments contained in the study reach, f_c was estimated from the observed concentration drop in the representative segment by means of an upscaling procedure (Equation (9)). To measure f_{c_r}, prior to each field measurement the stream bed was covered by a plastic film, to avoid lateral input of water and CO_2 and internal production induced by the ecosystem metabolism (Fig. S7). Then upstream vs

downstream CO_2 concentrations were measured under different hydrologic conditions (discharge range: from 0.19 to 2.11 l/s), and Equation (8) was applied. In the light of the constraint placed by the specific slope of the representative segment and the mean slope of the segments contained in the reach A, we analyzed three different scenarios, in which the damping factor of the reference segment was upscaled via Equation (9) referred to three different reaches: i) the whole reach A, which has a length L_A of $1060\,m$ and a mean slope of its continuous segments $i_{c,A}$ of $0.081\,m/m$; because $i_{c,A}$ is significantly smaller than the slope of ℓ_r, in this case f_c should be overestimated; ii) the reach B, including 130 steps, which has a length L_B equal to $543\,m$ and is characterized by an average slope of its continuous segments $i_{c,B} = 0.101\,m/m$ - quite close to the slope of the representative segment; iii) the reach A^*, an idealized reach characterized by: i) the same elevation drop as that observed in between the two endpoints of reach A; and ii) segments that have the same slope of the reference segment. A^* is $769\,m$ long, has a slope of its segments equal to $0.108\,m/m$ (by definition equal to $i_{c,r}$) and contains all the 271 steps of reach A (further details in SI). Since the mean slope of the segments included in B and A^* is closer to the actual slope of the reference segment, the corresponding estimates of f_c and r should be more reliable in this case. Note that the mean slope of the segments included in a reach was calculated starting from the mean slope of the overall reach, taking into account the heights of all the steps included in that reach and assuming a longitudinal size of $10\,cm$ for each step (SI). This implies that the length of the segments included in a reach is slightly smaller than the length of the whole reach (SI).

Morphological survey

The dominance ratio depends on the spatial frequency and the height distribution of the steps in the focus reach. We collected geometrical data about the step geometry during field surveys performed under very dry conditions. For each step we measured the step drop height, Δh, corresponding to the gap of water surface elevation in each nearly vertical fall with a drop higher than $10\,cm$. We mapped 271 steps in $1060\,m$ with an average Δh equal $23.7\,cm$ (Fig. S10). The frequency distribution of the step height was monotonically decreasing, with 47.6 % of steps in range $0 - 15\,cm$, and 70.5 % of steps in range $0 - 25\,cm$. Elevations, lengths and slopes of the relevant reaches were estimated through a high resolution ($1\,m$) *DTM*.

Streamflow regime

The streamflow regime was estimated from rainfall data using a simple rainfall-runoff model. In particular, we used daily precipitation heights P $[mm]$ recorded during the summer and fall seasons (Jun to October 2021) collected by a weather station of the Veneto Region Environmental Protection Agency (ARPAV) located in Falcade, 4.5 km far away from the catchment centroid. Discharge timeseries in the focus reach were then simulated using an exponential IUH

applied to the censored precipitation time series as:

$$Q(t) = A \sum_i j_i \, k \, e^{-k(t-t_i)} \ , \tag{11}$$

where A is the catchment area, k is the recession rate, t_i is the occurrence time of effective rain events, j_i is the effective (i.e. censored) rain depth ($j_i = max(P_i - \phi, 0)$, with P_i representing the total rain depth and ϕ the censoring threshold embedding soil moisture dynamics[52]. ϕ and k were calibrated against the discharge observations available (Figure 3c and SI).

Acknowledgments

This research was supported by the European Community's Horizon 2020 Excellent Science Programme (grant no. H2020-EU.1.1.-770999). The data that support the findings of this study are openly available in Botter et al., 2022[53] at http://researchdata.cab.unipd.it/id/eprint/619, reference number 619.

References

1. Cole, J. *et al.* Plumbing the global carbon cycle: integrating inland waters into the terrestrial carbon budget. *Ecosystems* **10,** 172–185 (2007).
2. Battin, T. *et al.* The boundless carbon cycle. *Nature Geoscience* **2,** 598–600 (2009).
3. Raymond, P. *et al.* Global carbon dioxide emissions from inland waters. *Nature* **503,** 355–359 (2013).
4. Drake, T. W., Raymond, P. A. & Spencer, R. G. Terrestrial carbon inputs to inland waters: A current synthesis of estimates and uncertainty. *Limnology and Oceanography Letters* **3,** 132–142 (2018).
5. Butman, D. & Raymond, P. Significant efflux of carbon dioxide from streams and rivers in the United States. *Nature Geoscience* **4,** 839–842 (2011).
6. Hotchkiss, E. *et al.* Sources of and processes controlling CO_2 emissions change with the size of streams and rivers. *Nature Geoscience* **8,** 696–699 (2015).
7. Duvert, C., Butman, D., Marx, A., Ribolzi, O. & Hutley, L. CO_2 evasion along streams driven by groundwater inputs and geomorphic controls. *Nature Geoscience* **11,** 813–818 (2018).
8. Horgby, Å. *et al.* Unexpected large evasion fluxes of carbon dioxide from turbulent streams draining the world's mountains. *Nature Communications* **10,** 1–9 (2019).
9. Leopold, L. B., Wolman, M. G. & Miller, J. P. *Fluvial processes in geomorphology* (USGS Publications Warehouse, New York, NY, 1964).

10. Chin, A. On the origin of step-pool sequences in mountain streams. *Geophysical research letters* **26,** 231–234 (1999).

11. Chin, A. & Wohl, E. Toward a theory for step pools in stream channels. *Progress in Physical Geography* **29,** 275–296 (2005).

12. Ashida, K., Takahashi, T. & Sawada, T. Sediment yield and transport on a mountainous small watershed. *Bulletin of the Disaster Prevention Research Institute* **26,** 119–144 (1976).

13. Abrahams, A. D., Li, G. & Atkinson, J. F. Step-pool streams: adjustment to maximum flow resistance. *Water resources research* **31,** 2593–2602 (1995).

14. Wohl, E., Madsen, S. & MacDonald, L. Characteristics of log and clast bed-steps in step-pool streams of northwestern Montana, USA. *Geomorphology* **20,** 1–10 (1997).

15. Montgomery, D. R. & Buffington, J. M. Channel-reach morphology in mountain drainage basins. *Geological Society of America Bulletin* **109,** 596–611 (1997).

16. Wohl, E. E. & Thompson, D. M. Velocity characteristics along a small step–pool channel. *Earth Surface Processes and Landforms: The Journal of the British Geomorphological Research Group* **25,** 353–367 (2000).

17. Chin, A. The geomorphic significance of step–pools in mountain streams. *Geomorphology* **55,** 125–137 (2003).

18. Comiti, F., Cadol, D. & Wohl, E. Flow regimes, bed morphology, and flow resistance in self-formed step-pool channels. *Water Resources Research* **45** (2009).

19. Wohl, E. & Jaeger, K. L. Geomorphic implications of hydroclimatic differences among step-pool channels. *Journal of hydrology* **374,** 148–161 (2009).

20. Cirpka, O., Reichert, P., Wanner, O., Mueller, S. R. & Schwarzenbach, R. P. Gas exchange at river cascades: field experiments and model calculations. *Environmental science & technology* **27,** 2086–2097 (1993).

21. Wallin, M. B. *et al.* Spatiotemporal variability of the gas transfer coefficient (KCO_2) in boreal streams: Implications for large scale estimates of CO_2 evasion. *Global Biogeochemical Cycles* **25** (2011).

22. Teodoru, C. R. *et al.* Dynamics of greenhouse gases (CO_2, CH_4, N_2O) along the Zambezi River and major tributaries, and their importance in the riverine carbon budget. *Biogeosciences* **12,** 2431–2453 (2015).

23. Marx, A. *et al.* A review of CO_2 and associated carbon dynamics in headwater streams: a global perspective. *Reviews of Geophysics* **55,** 560–585 (2017).

24. Rocher-Ros, G., Sponseller, R. A., Lidberg, W., Mörth, C.-M. & Giesler, R. Landscape process domains drive patterns of CO_2 evasion from river networks. *Limnology and Oceanography Letters* **4,** 87–95 (2019).

25. Ulseth, A. J. *et al.* Distinct air–water gas exchange regimes in low-and high-energy streams. *Nature Geoscience* **12,** 259–263 (2019).

26. Hall Jr, R. O. & Ulseth, A. J. Gas exchange in streams and rivers. *Wiley Interdisciplinary Reviews: Water* **7,** e1391 (2020).

27. Looman, A., Maher, D. T. & Santos, I. R. Carbon dioxide hydrodynamics along a wetland-lake-stream-waterfall continuum (Blue Mountains, Australia). *Science of The Total Environment* **777,** 146124 (2021).

28. Chan, C. N., Tsang, C. L., Lee, F., Liu, B. & Ran, L. Rapid loss of dissolved CO_2 from a subtropical steep headwater stream. *Frontiers in Earth Science* **9,** 996 (2021).

29. Natchimuthu, S., Wallin, M. B., Klemedtsson, L. & Bastviken, D. Spatio-temporal patterns of stream methane and carbon dioxide emissions in a hemiboreal catchment in Southwest Sweden. *Scientific reports* **7,** 1–12 (2017).

30. Leibowitz, Z. W., Brito, L. A. F., De Lima, P. V., Eskinazi-Sant'Anna, E. M. & Barros, N. O. Significant changes in water pCO_2 caused by turbulence from waterfalls. *Limnologica* **62,** 1–4 (2017).

31. Vautier, C. *et al.* Mapping gas exchanges in headwater streams with membrane inlet mass spectrometry. *Journal of Hydrology* **581,** 124398 (2020).

32. Schneider, C. L. *et al.* Carbon dioxide (CO_2) fluxes from terrestrial and aquatic environments in a high-altitude tropical catchment. *Journal of Geophysical Research: Biogeosciences* **125,** e2020JG005844 (2020).

33. Vidon, P. & Serchan, S. Impact of stream geomorphology on greenhouse gas concentration in a New York mountain stream. *Water, Air, & Soil Pollution* **227,** 1–13 (2016).

34. Hall Jr, R. O., Kennedy, T. A. & Rosi-Marshall, E. J. Air–water oxygen exchange in a large whitewater river. *Limnology and Oceanography: Fluids and Environments* **2,** 1–11 (2012).

35. Botter, G., Peruzzo, P. & Durighetto, N. Heterogeneity matters: aggregation bias of gas transfer velocity versus energy dissipation rate relations in streams. *Geophysical Research Letters* **48,** e2021GL094272 (2021).

36. Asher, W. E. & Wanninkhof, R. The effect of bubble-mediated gas transfer on purposeful dual-gaseous tracer experiments. *Journal of Geophysical Research: Oceans* **103,** 10555–10560 (1998).

37. Hall Jr, R. O. & Madinger, H. L. Use of argon to measure gas exchange in turbulent mountain streams. *Biogeosciences* **15,** 3085–3092 (2018).

38. Gameson, A. Weirs and the aeration of rivers. *J. Inst. Wat. Engrs* **11,** 477–490 (1957).

39. Gulliver, J. S., Thene, J. R. & Rindels, A. J. Indexing gas transfer in self-aerated flows. *Journal of Environmental Engineering* **116,** 503–523 (1990).

40. Moog, D. B. & Jirka, G. H. Stream reaeration in non uniform flow: macroroughness enhancement. *Journal of Hydraulic Engineering* **125(1),** 11–16 (1999).

41. Grant, G., Swanson, F. & Wolman, M. Pattern and origin of stepped-bed morphology in high-gradient streams, Western Cascades, Oregon. *Bulletin of the Geological Society of America* **102,** 340–352 (Mar. 1990).

42. D'Agostino, V. & Lenzi, M. A. Origine e dinamica della morfologia a gradinata (step pool) nei torrenti alpini ad elevata pendenza. *Dendronatura* **2,** 7–38 (1997).

43. Curran, J. & Wilcock, P. Characteristic dimensions of the step-pool bed configuration: An experimental study. *Water Resources Research* **41** (2005).

44. Wilcox, A., Wohl, E., Comiti, F. & Mao, L. Hydraulics, morphology, and energy dissipation in an alpine step-pool channel. *Water Resources Research* **47** (2011).

45. Chartrand, S., Jellinek, M., Whiting, P. & Stamm, J. Geometric scaling of step-pools in mountain streams: Observations and implications. *Geomorphology* **129,** 141–151 (2011).

46. Raymond, P. *et al.* Scaling the gas transfer velocity and hydraulic geometry in streams and small rivers. *Limnology and Oceanography: Fluids and Environments* **2,** 41–53 (2012).

47. Wallin, M. *et al.* Carbon dioxide and methane emissions of Swedish low-order streams - a national estimate and lessons learnt from more than a decade of observations. *Limnology and Oceanography Letters,* 156–167 (2018).

48. Liu, S. *et al.* The importance of hydrology in routing terrestrial carbon to the atmosphere via global streams and rivers. *Proceedings of the National Academy of Sciences* **119,** e2106322119 (2022).

49. Klaus, M., Labasque, T., Botter, G., Durighetto, N. & Schelker, J. Unraveling the Contribution of Turbulence and Bubbles to Air-Water Gas Exchange in Running Waters. *Journal of Geophysical Research: Biogeosciences* **127,** e2021JG006520 (2022).

50. Botter, G. & Durighetto, N. The stream length duration curve: a tool for characterizing the time variability of the flowing stream length. *Water Resources Research,* e2020WR027282 (2020).

51. Durighetto, N., Vingiani, F., Bertassello, L., Camporese, M. & Botter, G. Intraseasonal drainage network dynamics in a headwater catchment of the italian Alps. *Water Resources Research* **56,** e2019WR025563 (2020).

52. Botter, G., Porporato, A., Rodriguez-Iturbe, I. & Rinaldo, A. Basin-scale soil moisture dynamics and the probabilistic characterization of carrier hydrologic flows: Slow, leaching-prone components of the hydrologic response. *Water Resources Research* **43** (2007).

53. Botter, G., Carozzani, A., Peruzzo, P. & Durighetto, N. *Steps dominate gas evasion from a mountain headwater stream* (Research Data Unipd, Apr. 2022). http://researchdata.cab.unipd.it/619/.

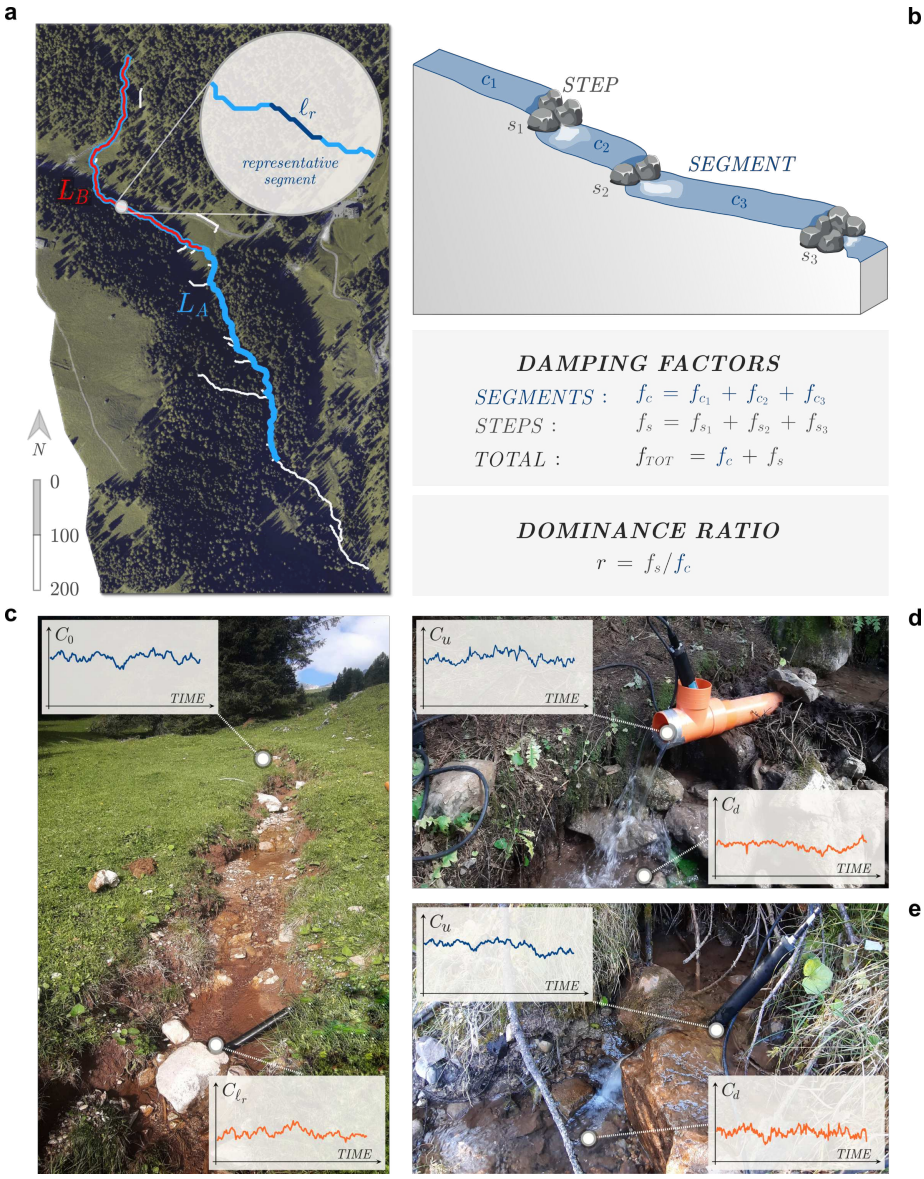

Figure 1: **Focus reach of the Valfredda creek and experimental set up**. a) planar view of the reach selected for this study, shown with an ortophoto of the eastern part of the Valfredda catchment in background. In particular, the reach A, with length $L_A = 1060\,m$, is indicated in light blue, while the reach B, with length $L_B = 543\,m$ is shown in red. The inset instead shows a planar view of the representative segment without steps, which has a length $\ell_r = 13\,m$; b) schematic of the decomposition of a reach into segments and steps, and aggregation of the damping factors f within a complex system, which leads to the definition of the dominance ratio r; c) overview of the reference segment, with the insets showing temporal dynamics of the water CO_2 concentration upstream (C_0) and downstream (C_{ℓ_r}) of the segment; d) artificial step, created by forcing the stream into a pipe, and then covering the downstream river bed with a plastic film; the insets show representative temporal dynamics of the water CO_2 concentration upstream (C_u) and downstream (C_d) of the step. e) same as d) but for a scoured natural step.

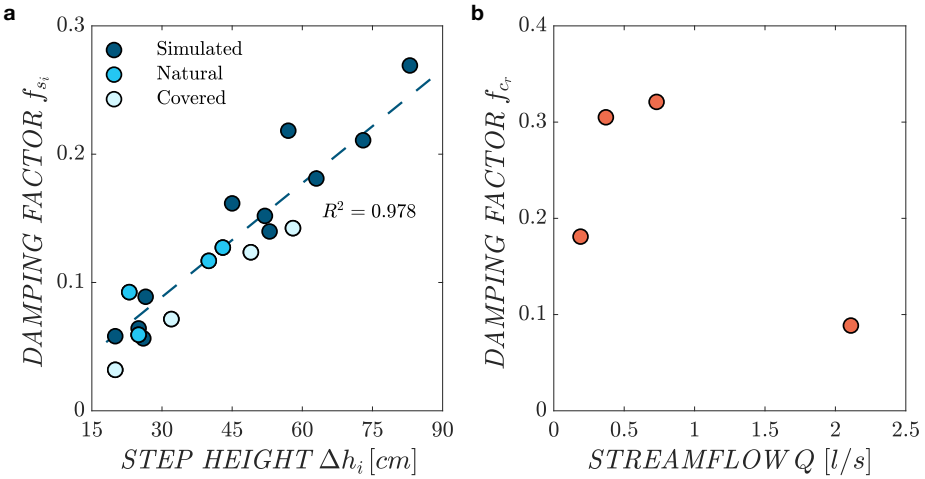

Figure 2: **Damping factors for the steps and the reference segment.** a) damping factor of the steps f_{s_i} as a function of the step height Δh_i for scoured natural steps (police strobe circles), natural covered steps (pale blue circles) and artificially simulated steps (navy blue circles). Also shown is the linear regression $f_{s_i} = 0.3\ \Delta h_i$ (with Δh_i in m), and the regression coefficient R^2; b) damping factor in the reference segment, f_{c_r}, for different discharge conditions in the range from 0.19 to 2.11 l/s.

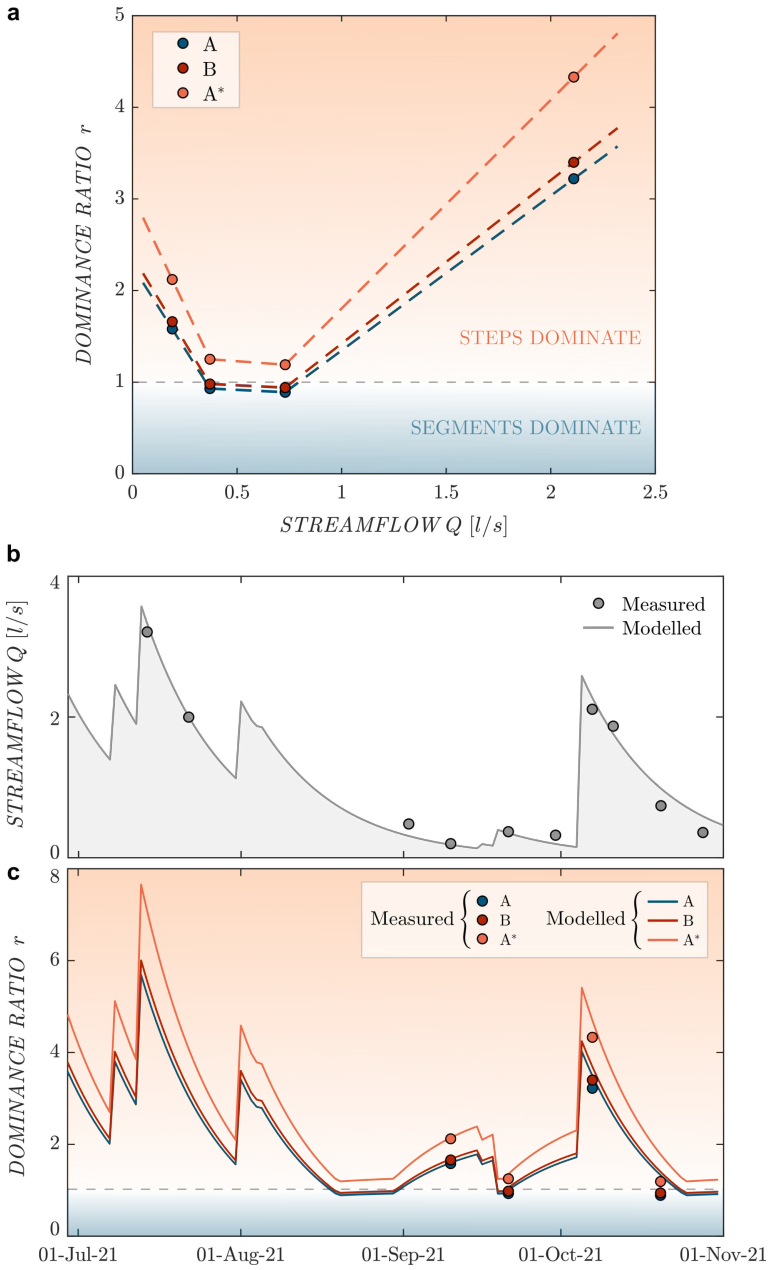

Figure 3: **Dominance ratio variations induced by changes in the underlying hydrologic conditions.** a) dominance ratio as a function of the stream discharge Q in the reaches A (blue petroleum), B (red) and A^* (orange). Circles represent the observed values of r, the dashed lines show a linear piece-wise interpolation. When $r > 1$ the steps dominate the outgassing (upper ibis-shaded region of the plot); b) temporal dynamics of the discharge in the reference segment of the focus reach from July 1 to Nov 1, 2021. Observed streamflows are indicated as grey dots, while the simulated discharges (see Methods) are shown by the shaded-grey region; c) temporal dynamics of the dominance ratio during the same time window shown in b) for the reaches A (blue petroleum), B (red) and A^* (orange). Circles refer to the observed values, while the solid lines refer to simulated values estimated based on the simulated discharges (shown in b) using the piece-wise linear interpolation between r and Q (shown in a). When $r > 1$ the steps dominate the outgassing (upper ibis-shaded region of the plot)

Supplementary Files

This is a list of supplementary files associated with this preprint. Click to download.

- SI.pdf